



## Antibacterial Properties of Green Silver Nanoparticles using Banana Peels Extract Loaded on Zeolite Clinoptilolite

Kek Jazz Yee<sup>1</sup>, Nik Ahmad Nizam Nik Malek<sup>2</sup>, Nurliyana binti Ahmad Zawawi<sup>1\*</sup>

<sup>1</sup>Department of Biosciences, Faculty of Science, Universiti Teknologi Malaysia, 81310 Johor Bahru, Johor, Malaysia

<sup>2</sup>Centre for Sustainable Nanomaterials (CSNano), Ibnu Sina Institute for Scientific and Industrial Research (ISI- ISIR), Universiti Teknologi Malaysia, 81310 Johor Bahru, Johor, Malaysia

\* e-mail: nurliyana@utm.my

### Abstract

Silver nanoparticles (AgNPs) have excellent antibacterial activity. However, the uses of AgNPs are limited due to unstable of AgNPs, and aggregation, leading to decreasing in antibacterial activity of AgNPs. This study aimed to synthesize and characterize banana peels extract silver nanoparticles-clinoptilolite (BPE-AgNPs-Cli) to improve antibacterial activity of AgNPs. BPE-AgNPs-Cli was confirmed successfully biosynthesized using UV-Vis spectrophotometer, Fourier Transform Infrared (FTIR), X-ray Diffraction (XRD), Scanning Electron Microscopy (SEM), Energy Dispersive X-ray (EDX), and dispersion behaviors test, compared to Cli, BPE-Cli and Ag-Cli. UV-Vis showed surface plasmon resonance peak at 430 nm. FTIR and XRD revealed incorporation of Ag<sup>+</sup> ions into clinoptilolite did not affect the original framework structure of clinoptilolite. SEM indicated BPE-AgNPs-Cli were irregular and smaller while EDX showed silver peak at 3 keV has been detected in BPE-AgNPs-Cli. BPE-AgNPs-Cli were good in dispersion. BPE-AgNPs-Cli exhibited its ability to inhibit bacterial growth in disc diffusion test as well as antibacterial activity against *Escherichia coli* (Gram-negative) and *Staphylococcus aureus* (Gram-positive) in distilled water and 0.9% saline solution in minimum inhibition concentration (MIC) and minimum bactericidal concentration (MBC) test. Antibacterial activity of BPE-AgNPs-Cli against bacteria proved its potential to be applied in biomedical fields in the future as good antibacterial carrier system.

**Keywords** Antibacterial activity; banana peels extract; clinoptilolite; green synthesis; silver nanoparticles

### Introduction

Due to its antibacterial, anti-inflammatory, anti-angiogenic, and catalytic activity (Panayotova et al., 2018), anticancer, antiviral, and larvicidal effects (Dutta et al., 2020), silver nanoparticles (AgNPs) are used frequently in biomedicine. However, the antibacterial activity of AgNPs is decreased which is attributed to their instability, the formation of larger AgNPs, and the ease with which the Ag<sup>+</sup> ions leached from the AgNPs (Mekki et al., 2021). Therefore, to retain the antibacterial action of AgNPs, many researchers proposed incorporating AgNPs into porous materials including zeolite (clinoptilolite), silica, and clay.

One of the zeolites that are prevalent in nature is clinoptilolite. Leaching and aggregation of AgNPs could be avoided by incorporating AgNPs into the clinoptilolite structure. As Dinler et al.

(2021) mentioned, the clinoptilolite framework consists of a trap-like cage structure and consistent pore size and shape which enable it to control the diffusion of AgNPs. This contributed to the clinoptilolite's quick ion-exchange capability and ability to restrict the mobility of AgNPs. Hence, the stability and antibacterial activity of AgNPs can be enhanced by entrapping AgNPs within the clinoptilolite framework or attach on its surface (Jou & Malek, 2016) to prevent the leaching of Ag<sup>+</sup> ions. Moreover, as many previous studies reported, banana peels extract consists of various reducing and capping agents like phenols and flavonoids, hence banana peels extract could be employed to reduce Ag<sup>+</sup> ions into AgNPs, and further stabilize the synthesized AgNPs.

Therefore, this study aimed to synthesize a green AgNP by using biomolecules of banana peels extract through the incorporation of Ag<sup>+</sup> ions into the clinoptilolite framework (BPE-AgNPs-Cli) to improve the antibacterial activity of AgNPs. The biosynthesized AgNPs were then characterized by UV-Visible (UV-Vis) spectrophotometer, Fourier Transform Infrared (FTIR) spectrophotometer, X-ray Diffraction (XRD), Scanning Electron Microscopy (SEM), Energy Dispersive X-ray (EDX), and dispersion behaviours test. While the antibacterial activity of BPE-AgNPs-Cli against *Escherichia coli* and *Staphylococcus aureus* was also performed in this study and compared to Cli, BPE-Cli, and Ag- Cli samples.

### Materials and methods

The synthesis method of BPE-AgNPs-Cli was adapted from the method used by (Asraf et al, 2020). About 2.0 g of clinoptilolite was mixed with 50 mL of 2.5 mM AgNO<sub>3</sub> solution and stirred overnight to completely mixed the solution. Next, 6.0 mL of BPE was added into the mixture and stirred for another 4 hours. To prepare BPE-Cli, 2.0 g of clinoptilolite was mixed with 50 mL of deionized water and stirred overnight. Next, 6.0 mL of BPE solution was added into the solution and then continuously stirred for another 4 hours. While Ag-Cli was prepared by mixing 2.0 g of clinoptilolite with 50 mL of 2.5 mM AgNO<sub>3</sub> solution and stirred overnight. After that, all sample mixture were filtered using Whatman filter paper. The residue was collected and dried in the oven at 70°C for 2 days. The completely dried powder was crushed and sieved to obtain the fine powder.

BPE-AgNPs was prepared following the method performed by (Kokila et al., 2015). 25 mL of 2.5 mM AgNO<sub>3</sub> solution was added into a 50 mL falcon tube and mixed with 3 mL of BPE solution. 28 mL of AgNO<sub>3</sub> solution and BPE solution were used as control. The samples were placed in the oven at 70°C for 72 hours. The colour changes was recorded and the synthesis of BPE-AgNPs was determined by using UV-Visible spectrophotometer (Jenway 7200) at 350- 750 nm.

BPE-AgNPs-Cli was characterized using Fourier Transform Infrared (FTIR) spectrophotometer, X-ray diffraction (XRD), Scanning Electron Microscopy (SEM), Energy Dispersive X-ray (EDX), and dispersion behaviour test in comparison with Cli, BPE-Cli, and Ag-Cli to confirm the successful incorporation of AgNPs into the clinoptilolite structure. FTIR was used to identify the possible functional groups present in the samples while XRD analysed the crystalline structures of the samples. To study the surface morphology, size and elemental composition of the samples, SEM and EDX were conducted. Dispersion behaviour test was carried out to investigate the relative position of BPE- AgNPs-Cli in oil-water mixture.

The antibacterial activity of BPE-AgNPs-Cli was studied against Gram-negative bacteria, *Escherichia coli* ATCC 11229 and Gram-positive bacteria, *Staphylococcus aureus* ATCC 6538 using disc diffusion test (DDT), and minimum inhibition concentration (MIC) and minimum bactericidal concentration (MBC). DDT was carried out following the method performed by (Jou & Malek, 2016) to determine the zone of inhibition formed by the samples. About 0.3 g of the samples were weighted and pressed using Manual Hydraulic Pellet Press to prepare pellet samples. 5- 10 colonies of *E. coli* and *S. aureus* were taken and transferred to 5 mL of sterile 0.9 % (w/v) saline solution. The turbidity test of the bacterial suspension was compared with McFarland Standard ( $1.5 \times 10^8$  cells). The sterile cotton swab was dipped into the bacterial suspension and inoculated on the surface of MHA plates by rotating the plates every 60° for 6 times to make sure the bacterial suspension was spread uniformly on the agar surface. Then, the pellet samples were placed on top of the agar and incubated at 37°C overnight upsides down. After incubation, the zone of inhibition was measured (in cm) using

a ruler.

For MIC/ MBC analysis, it was adapted from (Jou & Malek, 2016). 100 mL of bacterial suspension which was in log phase was divided into two 50 mL bacterial suspension for distilled water and 0.9 % saline solution tests, then centrifuged at 4000 rpm for 15 minutes. The pellets were collected by discarding the supernatants and washed with distilled water and 0.9 % saline solution respectively twice. The pellets were resuspended in 350 mL distilled water and 0.9 % saline solution. Next, Cli, Ag- Cli, BPE-AgNPs-Cli, and BPE-Cli samples with different weights (0.005, 0.010, 0.020, 0.050, 0.080, and 0.100 g) are added into 10 mL of the bacterial cell suspensions to form a series of different concentrations (0.5, 1.0, 2.0, 5.0, 8.0, and 10.0 g/ mL). The mixtures were incubated using the incubator shaker at 100 rpm for 30 minutes. 100  $\mu$ L of 50 mg/ mL kanamycin sulphate was used as positive control while bacteria were used as negative control. After that, 10  $\mu$ L of each suspension was dropped into the MHA plate by drop plate method. The plates were incubated at 37°C overnight and observed for any colony formation. MIC value of the samples was the lowest concentration that inhibited bacterial growth while MBC value of the samples was the lowest concentration that killed all bacteria.

### Results and discussion

BPE-AgNPs were prepared in this study to determine the use of BPE to reduce Ag<sup>+</sup> ions to AgNPs was a more eco-friendly, and cost-effective method. AgNO<sub>3</sub> solution changed from colourless to light yellow after adding BPE, and further changed to dark brown after placing in the oven for 72 hours (Figure 1). The colour changes were due to the reduction of Ag<sup>+</sup> ions into AgNPs (Ag<sup>0</sup>) by biomolecules of BPE like phenolics and flavonoids (Ruangtong et al., 2020). The functional groups of phenolics and flavonoids interact with Ag<sup>+</sup> ions and promote the reduction of Ag<sup>+</sup> ions to AgNPs while C=O, C=O–C, and C–C groups that present in the heterocyclic compounds act to stabilize the biosynthesized AgNPs (Hussain et al., 2019).

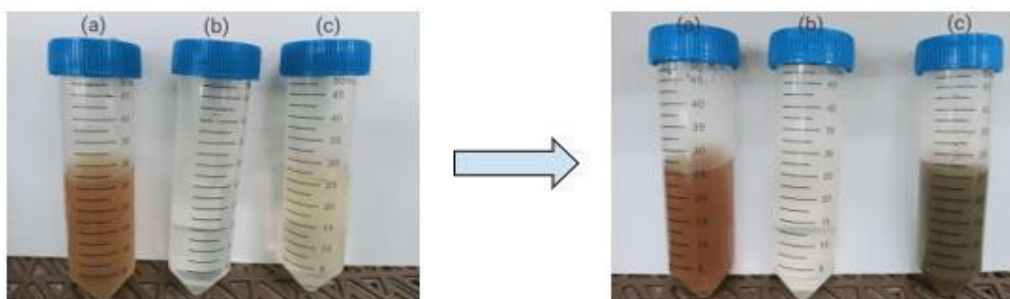


**Figure 1** Biosynthesis of BPE-AgNPs after 72 hours: (a) banana peels extract (BPE); (b) silver nitrate AgNO<sub>3</sub>; (c) banana peels extract silver nanoparticles (BPE-AgNPs)

The successful formation of BPE-AgNPs was further confirmed by UV-Vis spectrophotometer. Figure 2 shows UV-Visible spectra with the absorbance of AgNO<sub>3</sub>, BPE and BPE-AgNPs at a wavelength between 350 nm to 750 nm. A strong SPR band formed at 430 nm with broad peak indicates the AgNPs synthesized in the solution are spherical (Kokila et al., 2015). Additionally, a single SPR peak was observed which also confirmed the spherical BPE-AgNPs was formed. Kokila et al. (2015) stated the spherical AgNPs only display a single SPR band in absorption spectra. The broad peak represents the AgNPs are monodispersed. In contrast, AgNO<sub>3</sub> and BPE acted as controls and did not show any characteristic peaks.

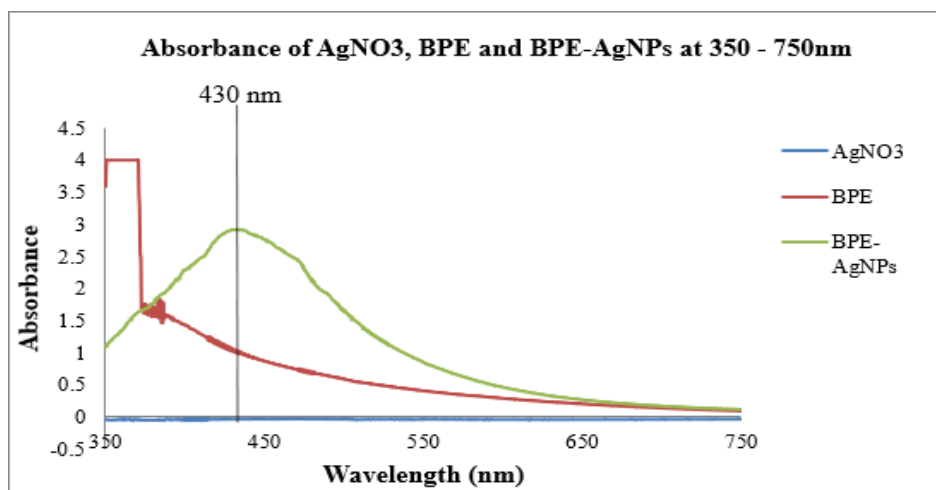


**Figure 2** UV-Vis spectrophotometer: absorbance of AgNO<sub>3</sub>, BPE and BPE-AgNPs at 350-750 nm.

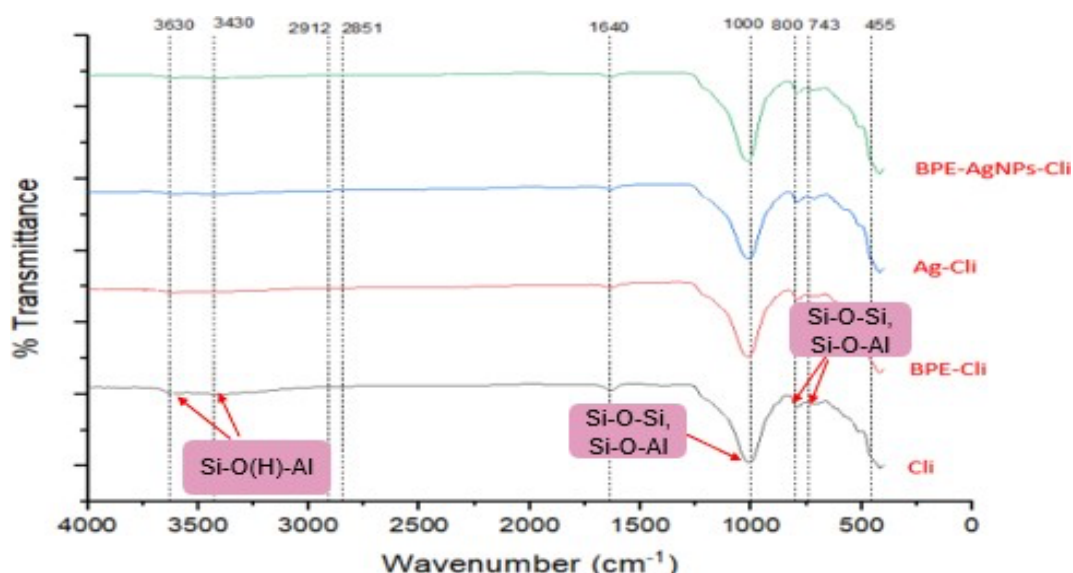


**Figure 3** FTIR spectra of Cli, BPE-Cli, Ag-Cli, and BPE-AgNPs-Cli

To confirm the successful synthesis of BPE-AgNPs-Cli, FTIR was performed between a range of 4000 to 400  $\text{cm}^{-1}$  to characterize the functional groups that present in BPE-AgNPs-Cli, compared to Cli, BPE-Cli, and Ag-Cli (Figure 3). FTIR spectra indicated a strong band of clinoptilolite asymmetric stretching of Si-O-Si and Si-O-Al at around 1000  $\text{cm}^{-1}$ . According to Hrenovic et al. (2011), two medium bands formed at 800  $\text{cm}^{-1}$  and 743  $\text{cm}^{-1}$  were assigned to the symmetric stretching of Si-O-Si and Si-O-Al of clinoptilolite. At 3630  $\text{cm}^{-1}$  and 3430  $\text{cm}^{-1}$ , the weak bands that represented the acidic hydroxyl groups of Si-O(H)-Al was found due to vibration of the O-H bonds respectively (Mortazavi et al., 2021). A formation of a broad peak at 455  $\text{cm}^{-1}$  which indicated the bending vibrations of Si-O and Al-O, while a band found at 1640  $\text{cm}^{-1}$  is resulting from the deformation vibration of absorbed water (Mortazavi et al., 2021). BPE-AgNPs-Cli showed similar bands and functional groups as the raw clinoptilolite. This revealed the Ag<sup>+</sup> ions were ion-

exchanged with cations in the clinoptilolite framework but did not affect and disrupt the original clinoptilolite structure (Hrenovic et al., 2011). However, a band represented C-H in alkanes and N-H in amines that were expectedly present in BPE-AgNPs-Cli at around  $2851$  to  $2912\text{ cm}^{-1}$  was not found. This may be because of the low content of BPE in BPE-AgNPs-Cli which is difficult to be detected in FTIR.

Figure 4 displayed the XRD pattern to determine the crystalline size and structure of BPE-AgNPs-Cli in comparison with Cli, BPE-Cli, and Ag-Cli. The major clinoptilolite peaks were detected in BPE-AgNPs-Cli at  $11.12^\circ$ ,  $13.51^\circ$ ,  $15.27^\circ$ ,  $17.26^\circ$ ,  $19.64^\circ$ ,  $22.24^\circ$ ,  $23.60^\circ$ ,  $25.67^\circ$ ,  $27.78^\circ$ ,  $29.51^\circ$ ,  $30.93^\circ$ ,  $35.66^\circ$ , and  $48.58^\circ$ . From the figure, it can be seen that BPE-AgNPs-Cli indicated a similar peak as the raw clinoptilolite. This proved the  $\text{Ag}^+$  ions were attached to the clinoptilolite surface without affecting and changing the original clinoptilolite structure or intercalating between the clinoptilolite layers (Jou & Malek, 2016). Moreover, BPE-AgNPs-Cli also contained organic compounds of BPE which act as reducing and capping agents in the biosynthesis of AgNPs since the peaks were formed at  $32.25^\circ$  and  $46.16^\circ$  (Ibrahim, 2015). The silver peak was supposedly detected at  $38.03^\circ$  and  $44.05^\circ$  which correspond to the (1 1 1) and (2 0 0) planes of silver (Dat et al., 2021), however, there was no silver peak found in BPE-AgNPs-Cli. The incomplete reduction of  $\text{AgNO}_3$  to AgNPs (Dat et al., 2021) and the low amount of  $\text{Ag}^+$  ions contained in BPE-AgNPs-Cli may lead to the difficulty to detect silver peaks.

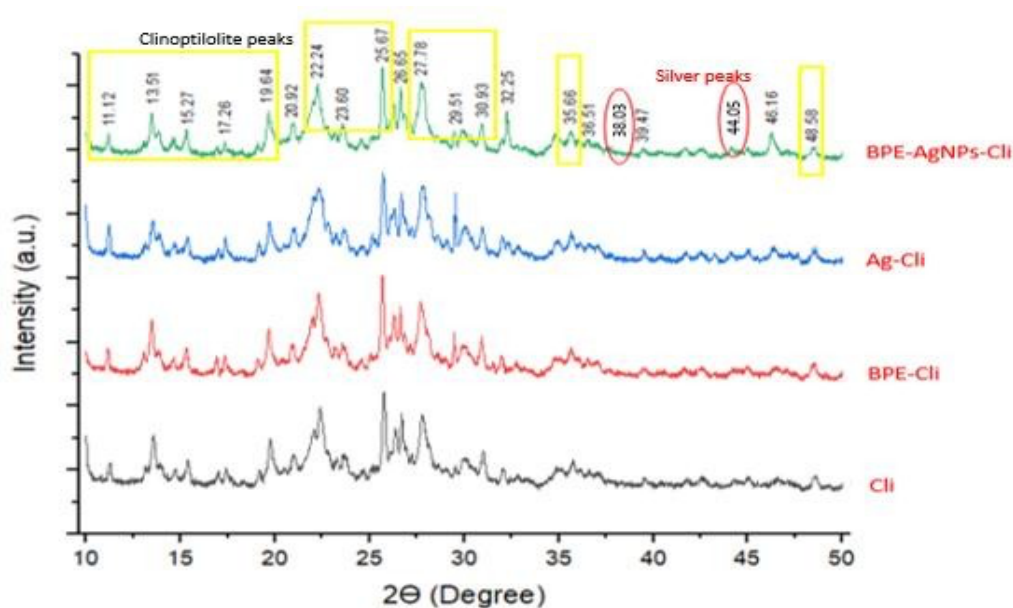


**Figure 4** Diffractogram of Cli, BPE-Cli, Ag-Cli, and BPE-AgNPs-Cli

SEM was carried out to analyze the surface morphology and size of BPE-AgNPs-Cli compared to Cli, BPE-Cli, and Ag-Cli. SEM images showed the natural clinoptilolite was spherical and consisted of a highly porous structure (Figure 5) which created the negatively charged channels for ion-exchange of  $\text{Ag}^+$  ions with cations into the clinoptilolite structure (Copcica et al., 2011). However, BPE-AgNPs-Cli was not comparable to the natural clinoptilolite as the SEM images for both samples were caught from different regions and different angles. BPE-AgNPs-Cli was found to be irregular and smaller in size due to the 24-hour treatment of BPE-AgNPs-Cli in  $\text{AgNO}_3$  solution decreased the size of the clinoptilolite structure (Panayotova et al., 2018), and also resulting from mechanical processes such as grinding and mixing (Dikmen et al., 2020). Additionally, the pore system of clinoptilolite cannot be observed on the surface of BPE-AgNPs-Cli,

which may be because of the formation of silver clusters during the process partially blocked the pore system (Panayotova et al., 2018). Moreover, the low resolution of SEM cause the Ag<sup>+</sup> ions and AgNPs cannot be detected and observed on the clinoptilolite surface.

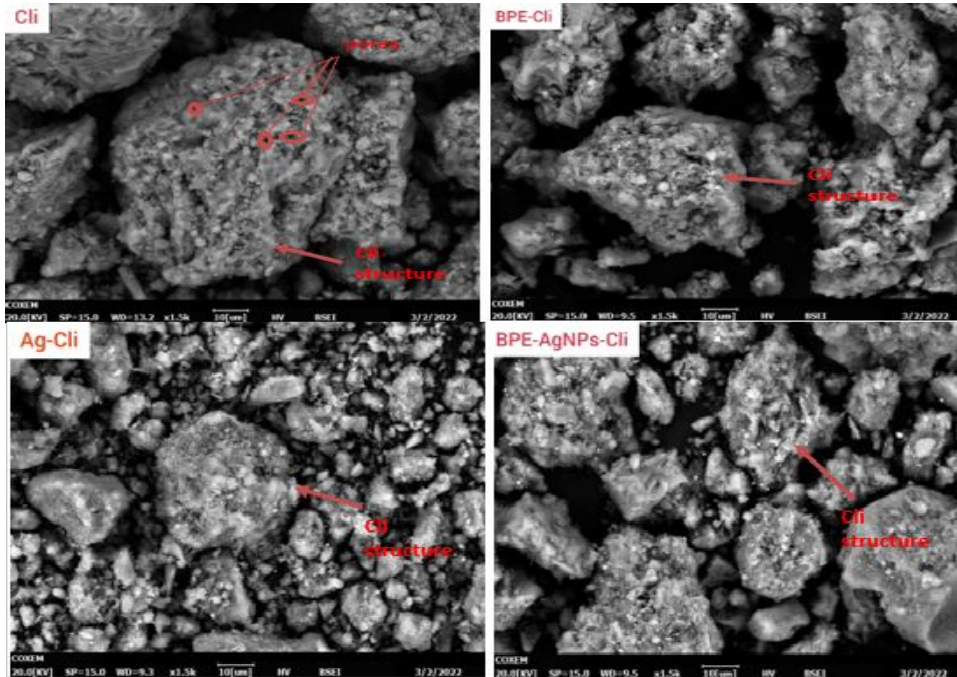


**Figure 5** SEM images of Cli, BPE-Cli, Ag-Cli, and BPE-AgNPs-Cli

To determine the elemental compositions of BPE-AgNPs-Cli, EDX was performed, compared to Cli, BPE-Cli, and Ag-Cli. Referring to Figure 6, EDX spectra indicated BPE-AgNPs-Cli contained major elements found in clinoptilolite, including silica (Si), aluminium (Al), and oxygen (O). Among these elements, a strong peak that represents the Si element was observed at 1.7 keV. Cations such as K<sup>+</sup>, Ca<sup>2+</sup> and Mg<sup>2+</sup> ions that present within clinoptilolite structure were also found in BPE-AgNPs-Cli, which function to exchange with Ag<sup>+</sup> ions for AgNPs-Cli synthesis.

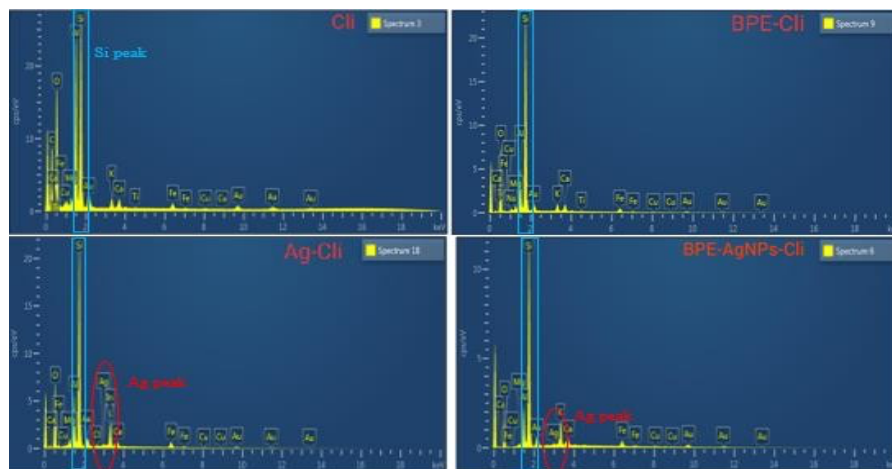


















**Figure 6** EDX spectra of Cli, BPE-Cli, Ag-Cli, and BPE-AgNPs-Cli

Apart from clinoptilolite elements, silver (Ag) element was detected with a peak at 3 keV. According to Ansar et al. (2020), the surface plasmon resonance of the Ag<sup>+</sup> ions led to a silver signal formed at 3 keV. The detection of Ag peak in BPE-AgNPs-Cli proved Ag<sup>+</sup> ions were successfully incorporated into the clinoptilolite framework. The quantitative analysis of elemental compositions of BPE-AgNPs-Cli was shown in Table 1 in comparison with Cli, BPE-Cli, and Ag-Cli. It was found that BPE-AgNPs-Cli consisted of 37.97 % silica, followed by 32.87 % oxygen, 6.90 % aluminium, and 1.24 % silver.

**Table 1:** Elemental composition of Cli, BPE-Cli, Ag-Cli, and BPE-AgNPs-Cli by EDX analysis

Samples	Weight of major elements (%)							
	O	C	Si	Al	K	Ca	Mg	Ag
<b>Cli</b>	41.52	32.06	11.20	9.46	0.74	0.76	0.55	-
<b>BPE-Cli</b>	46.50	-	33.07	6.97	1.83	1.90	0.94	-
<b>Ag-Cli</b>	45.55	-	29.64	7.24	4.73	0.88	1.22	1.28
<b>BPE-AgNPs-Cli</b>	32.87	-	37.97	6.90	6.80	1.87	0.48	1.24

**Table 2** Dispersion behaviour test for Cli, BPE-Cli, Ag-Cli, and BPE-AgNPs-Cli samples in oil-watermixture

Samples	Before shaking	After shaking	Left in static condition for 30 mins	Left in static condition for 24 hours
Cli				
BPE-Cli				
Ag-Cli				
BPE-AgNPs-Cli				

Dispersion behaviour test was conducted to investigate the dispersibility and relative position of BPE-AgNPs-Cli powder in an oil-water mixture, compared to Cli, BPE-Cli, and Ag-Cli. The successful incorporation of Ag<sup>+</sup> ions into the clinoptilolite framework was also can be confirmed by this dispersion test. The dispersibility of Cli, BPE-Cli, Ag-Cli, and BPE-AgNPs-Cli in hexane and water mixture before and after shaking, and left in static condition for 30 minutes and 24 hours were shown in Table 2.

Before shaking, Cli started to distribute to the bottom of the bottle due to water shells forming a barrier between the clinoptilolite particles, leading to dispersion of clinoptilolite particles (Jou & Malek, 2016) while BPE-AgNPs-Cli was present in the interface phase between hexane and water mixture. BPE-AgNPs-Cli were dispersed in the water phase after shaking, which indicated they have well dispersibility to transport to different phases of the solution and evenly distribute throughout the solution. Then, BPE-AgNPs-Cli was distributed to lower level of the water phase after being left at static condition for 30 minutes. Because of the gravitational force, BPE-AgNPs-Cli was dispersed in the bottom of the bottle after 24 hours. This showed the successful incorporation of BPE-AgNPs-Cli into clinoptilolite structure, hence, eventually they presented as a solid powder at the bottom of the bottles.

Antibacterial activity of BPE-AgNPs-Cli was analyzed against *Escherichia coli* and *Staphylococcus aureus* by disc diffusion test in comparison with Cli, BPE-Cli, and Ag-Cli (Figure 7). Due to Cli and BPE-Cli did not contain any antibacterial agent, they did not show their antibacterial activity against *E. coli* and *S. aureus*. There was no visible inhibition zone formed around Cli and BPE-Cli pellet samples for both *E. coli* and *S. aureus*. In contrast, it can be seen that a clear inhibition zone was formed around Ag-Cli and BPE-AgNPs-Cli pellet samples for both *E. coli* and *S. aureus*. This proved that BPE-AgNPs-Cli exhibited antibacterial activity against *E. coli* and *S. aureus*. BPE-AgNPs-Cli was composed of clinoptilolite particles that incorporated with Ag<sup>+</sup> ions which have antibacterial activity. As Azizi-Lalabadi et. al. (2021) reported, the release of Ag<sup>+</sup> ions and AgNPs to interact with bacteria was controlled by the ion exchange and pore system of clinoptilolite. Hence, the Ag<sup>+</sup> ions and AgNPs in BPE-AgNPs-Cli could be released into the culture medium and inhibit bacterial growth by forming a clear zone of inhibition.



**Figure 7** Antibacterial activity of Cli, BPE-Cli, Ag-Cli, and BPE-AgNPs-Cli against *E. coli* (left) and *S. aureus* (right) by disc diffusion test

The zone of inhibition formed against *E. coli* and *S. aureus* was measured and recorded in Table 3. BPE-AgNPs-Cli showed a growth inhibition zone of 0.2 cm against *E. coli* and 0.3 cm against *S. aureus*. The results indicated the inhibition zone formed against *S. aureus* was slightly larger than *E. coli*, which means BPE-AgNPs-Cli exhibited higher antibacterial activity against *S. aureus* (Gram-positive bacteria) than *E. coli* (Gram-negative bacteria). This is due to the peptidoglycan layer of Gram-positive bacteria cell wall consisting of teichoic acid and pore system,



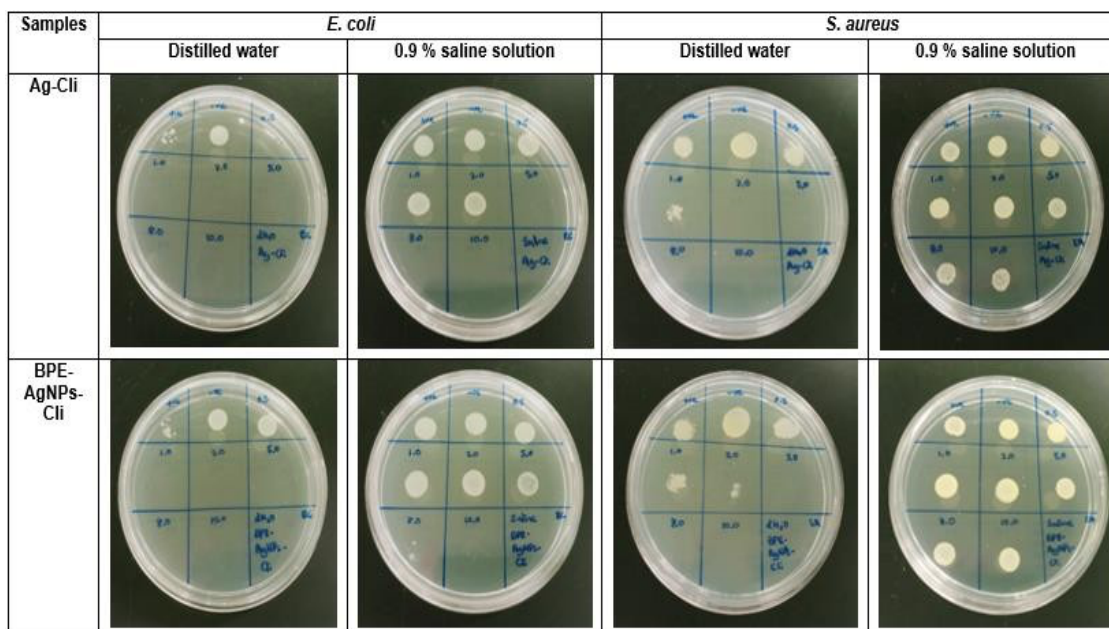
which facilitate Ag<sup>+</sup> ions and AgNPs to easily penetrate into the bacterial cells, disrupt bacterial DNA and protein, and lead to cell death or apoptosis (Wang et al., 2017). Instead, Gram-negative bacteria cell wall was composed of lipopolysaccharides and lipoproteins which will block the Ag<sup>+</sup> ions and AgNPs from entering the bacterial cells, thus BPE-AgNPs-Cli was less effective against *E. coli* (Loo et al., 2018).

**Table 3** Measurement of zone of inhibition (cm) of disc diffusion test for *E. coli* and *S. aureus*

Samples	Zone of inhibition (cm)	
	<i>E. coli</i>	<i>S. aureus</i>
Cli	-	-
BPE-Cli	-	-
Ag-Cli	0.3 ± 0.05	0.4 ± 0.05
BPE-AgNPs-Cli	0.2 ± 0.05	0.3 ± 0.05

Minimum inhibition concentration (MIC) and minimum bactericidal concentration (MBC) tests were performed to determine the lowest concentration of BPE-AgNPs-Cli required to inhibit the bacterial growth and completely kill the bacteria. In this study, the antibacterial activity of BPE-AgNPs-Cli against *E. coli* and *S. aureus* was conducted in distilled water and 0.9% saline solution to evaluate the effectiveness of antibacterial activity of BPE-AgNPs-Cli after incorporation of Ag<sup>+</sup> ions and AgNPs into clinoptilolite structure. As previously discussed in the disc diffusion test, Cli and BPE-Cli did not contain antibacterial agents to inhibit bacterial growth and kill *E. coli* and *S. aureus*. In contrast, Ag-Cli and BPE-AgNPs-Cli exhibited their antibacterial activity against *E. coli* and *S. aureus* in distilled water and 0.9% saline solution (Table 4).

**Table 4** Antibacterial activity of Ag-Cli, and BPE-AgNPs-Cli against *E. coli* and *S. aureus* in distilled water and 0.9 % saline solution by MIC / MBC test



MIC/MBC values of BPE-AgNPs-Cli against *E. coli* and *S. aureus* in distilled water and 0.9 % saline solution were shown in Table 5, compared to Cli, BPE-Cli, and Ag-Cli. It can be seen that 1.0 g/mL and 10.0 g/mL of BPE-AgNPs-Cli were able to inhibit bacterial growth and kill *E. coli* in

distilled water and 0.9% saline solution respectively. While for *S. aureus*, 5.0 g/mL and more than 10.0 g/mL of BPE-AgNPs-Cl<sub>i</sub> were required to inhibit and completely kill the bacterial growth in distilled water and 0.9% saline solution respectively.

**Table 5** MIC / MBC values of Cl<sub>i</sub>, BPE-Cl<sub>i</sub>, Ag-Cl<sub>i</sub>, and BPE-AgNPs-Cl<sub>i</sub> against *E. coli* and *S. aureus* indistilled water and 0.9 % saline solution

Samples	MIC				MBC			
	<i>E. coli</i>		<i>S. aureus</i>		<i>E. coli</i>		<i>S. aureus</i>	
	Distilled water	0.9 % saline solution	Distilled water	0.9 % saline solution	Distilled water	0.9 % saline solution	Distilled water	0.9 % saline solution
Cl <sub>i</sub>	> 10.0 *	> 10.0 *	> 10.0 *	> 10.0 *	> 10.0 *	> 10.0 *	> 10.0 *	> 10.0 *
BPE-Cl <sub>i</sub>	> 10.0 *	> 10.0 *	> 10.0 *	> 10.0 *	> 10.0 *	> 10.0 *	> 10.0 *	> 10.0 *
Ag-Cl <sub>i</sub>	0.5	5.0	0.5	5.0	0.5	5.0	2.0	> 10.0
BPE-AgNPs-Cl <sub>i</sub>	1.0	5.0	0.5	5.0	1.0	10.0	5.0	> 10.0

Notes: \* represent the sample that does not possess antibacterial activity

BPE-AgNPs-Cl<sub>i</sub> demonstrated its antibacterial activity against *E. coli* and *S. aureus* in distilled water and 0.9% saline solution since it can inhibit the bacterial colonies formed on the agar. Ag<sup>+</sup> ions and AgNPs in BPE-AgNPs-Cl<sub>i</sub> were released from the clinoptilolite structure to act as antibacterial agents when interacting with bacteria. They bind to bacterial cell walls and damage the cell membrane, leading to an increase in permeability of the cell membrane and leaking of intracellular components, even cell death (Kanniah et al., 2021). Furthermore, it can be seen that BPE-AgNPs-Cl<sub>i</sub> exhibited higher antibacterial activity against *E. coli* and *S. aureus* in distilled water than in 0.9% saline solution, which is due to the precipitation of silver chloride. The released Ag<sup>+</sup> ions may react with Cl<sup>-</sup> ions in saline solution and formed silver chloride precipitate, causing a decrease in the number of Ag<sup>+</sup> ions to interact with bacteria and inhibit bacterial growth (Jou & Malek, 2016). Hence, the results indicated a slightly diminished antibacterial activity of BPE-AgNPs-Cl<sub>i</sub> against *E. coli* and *S. aureus* in 0.9 % saline solution.

## Conclusion

BPE-AgNPs-Cl<sub>i</sub> was successfully synthesized through the incorporation of Ag<sup>+</sup> ions into clinoptilolite structure, and reduced into AgNPs by biomolecules of banana peel extracts. The successful synthesis of BPE-AgNPs-Cl<sub>i</sub> was confirmed by UV-Vis, FTIR, XRD, SEM, EDX, and dispersion behaviour test. Antibacterial assay showed BPE-AgNPs-Cl<sub>i</sub> was able to inhibit the bacterial growth of *E. coli* and *S. aureus* in DDT, and also exhibited its antibacterial activity in distilled water and 0.9 % saline solution in MIC/MBC test. Therefore, BPE-AgNPs-Cl<sub>i</sub> has the potential to be applied as a new antibacterial agent in biomedical field and further study is required for more exploration in its properties and optimal conditions for the preparation of BPE-AgNPs-Cl<sub>i</sub>.

## Acknowledgement

The authors would like to acknowledge Ministry of Higher Education (MOHE) and Universiti Teknologi Malaysia (Encouragement Grant, Tier-2 No. Q.J130000.2645.15J81) for financial support.

## References

- Ansar, S., Tabassum, H., Aladwan, N. S. M., Ali, M. N., Almaarik, B., Mahrouqi, S. A., Abudawood, M., Banu, N. & Alsubki, R. (2020). Eco friendly silver nanoparticles synthesis by *Brassica oleracea* and its antibacterial, anticancer and antioxidant properties. *Scientific Reports* (2020) 10, 18564. <https://doi.org/10.1038/s41598-020-74371-8>
- Asraf, M. H., Sani, N. S., Williams, C. D., Jemon, K., & Malek, N. A. N. N. (2021). In situ biosynthesized silver nanoparticle-incorporated synthesized zeolite A using *Orthosiphon aristatus* extract for in vitro antibacterial wound healing. *Particuology*. <https://doi.org/10.1016/j.partic.2021.09.007>
- Azizi-Lalabadi, M., Garavand, F., & Jafari, S. M. (2021). Incorporation of silver nanoparticles into active antimicrobial nanocomposites: Release behavior, analyzing techniques, applications and safety issues. *Advances in Colloid and Interface Science*, 293, 102440. <https://doi.org/10.1016/j.cis.2021.102440>
- Copcia, V. E., Luchian, C., Dunca, S., Bilba, N., & Hristodor, C. M. (2011). Antibacterial activity of silver-modified natural clinoptilolite. *Journal of Materials Science*, 46(22), 7121-7128. <https://doi.org/10.1007/s10853-011-5635-0>
- Dat, T. Do, Viet, N. D., Dat, N. M., My, P. L. T., Thinh, D. B., Thy, L. T. M., Huong, L. M., Khang, P. T., Hai, N. D., Nam, H. M., Phong, M. T., & Hieu, N. H. (2021). Characterization and bioactivities of silver nanoparticles green synthesized from Vietnamese *Ganoderma lucidum*. *Surfaces and Interfaces*, 27(September), 101453. <https://doi.org/10.1016/j.surfin.2021.101453>
- Dikmen, S., Şahin, N., Dikmen, Z. & Tanışlı, M. (2020). Characterization of Ag-exchanged clinoptilolite treated with a plasma jet at atmospheric pressure. *Clay Minerals* 55, 238–247. <https://doi.org/10.1180/clm.2020.33>
- Dinler, A. C., Voyvoda, H., Ulutas, P. A., Karagenc, T., & Ulutas, B. (2021). Prophylactic and therapeutic efficacy of clinoptilolite against *Cryptosporidium parvum* in experimentally challenged neonatal lambs. *Veterinary Parasitology*, 299(August), 109574. <https://doi.org/10.1016/j.vetpar.2021.109574>
- Dutta, T., Ghosh, N. N., Das, M., Adhikary, R., Mandal, V., & Chattopadhyay, A. P. (2020). Green synthesis of antibacterial and antifungal silver nanoparticles using *Citrus limetta* peel extract: Experimental and theoretical studies. *Journal of Environmental Chemical Engineering*, 8(4), 104019. <https://doi.org/10.1016/j.jece.2020.104019>
- Hrenovic, J., Milenkovic, J., Ivankovic, T., & Rajic, N. (2012). Antibacterial activity of heavy metal-loaded natural zeolite. *Journal of Hazardous Materials*, 201–202, 260-264. <https://doi.org/10.1016/j.jhazmat.2011.11.079>
- Hussain, A., Alajmi, M. F., Khan, M. A., Pervez, S. A., Ahmed, F., Amir, S., Husain, F. M., Khan, M. S., Shaik, G. M., Hassan, I., Khan, R. A., & Rehman, M. T. (2019). Biosynthesized silver nanoparticle (AgNP) from *pandanus odorifer* leaf extract exhibits anti-metastasis and anti-biofilm potentials. *Frontiers in Microbiology*, 10(FEB), 1–19. <https://doi.org/10.3389/fmicb.2019.00008>
- Ibrahim, H. M. M. (2015). Green synthesis and characterization of silver nanoparticles using banana peel extract and their antimicrobial activity against representative microorganisms. *Journal of Radiation Research and Applied Sciences*, 8(3), 265–275. <https://doi.org/10.1016/j.jrras.2015.01.007>
- Jou, S. K., & Malek, N. A. N. N. (2016). Characterization and antibacterial activity of chlorhexidine loaded silver-kaolinite. *Applied Clay Science*, 127–128, 1-9.
- Kanniah, P., Chelliah, P., Thangapandi, J. R., Gnanadhas, G., Mahendran, V., & Robert, M. (2021). Green synthesis of antibacterial and cytotoxic silver nanoparticles by *Piper nigrum* seed extract and development of antibacterial silver based chitosan nanocomposite. *International Journal of Biological Macromolecules*, 189(August), 18–33. <https://doi.org/10.1016/j.ijbiomac.2021.08.056>
- Kokila, T., Ramesh, P. S., & Geetha, D. (2015). Biosynthesis of silver nanoparticles from *Cavendish*

- banana peel extract and its antibacterial and free radical scavenging assay: a novel biological approach. *Applied Nanoscience (Switzerland)*, 5(8), 911–920. <https://doi.org/10.1007/s13204-015-0401-2>
- Loo, Y. Y., Rukayadi, Y., Nor-Khaizura, M. A. R., Kuan, C. H., Chieng, B. W., Nishibuchi, M., & Radu, S. (2018). In Vitro antimicrobial activity of green synthesized silver nanoparticles against selected Gram-negative foodborne pathogens. *Frontiers in Microbiology*, 9(JUL), 1–7. <https://doi.org/10.3389/fmicb.2018.01555>
- Mekki, A., Mokhtar, A., Hachemaoui, M., Beldjilali, M., Meliani, M. fethia, Zahmani, H. H., Hacini, S., & Boukoussa, B. (2021). Fe and Ni nanoparticles-loaded zeolites as effective catalysts for catalytic reduction of organic pollutants. *Microporous and Mesoporous Materials*, 310(July 2020), 110597. <https://doi.org/10.1016/j.micromeso.2020.110597>
- Mortazavi N., Bahadori M., Marandi A., Tangestaninejad S., Moghadam M., Mirkhani V., Mohammadpoor B. I. (2021). Enhancement of CO<sub>2</sub> adsorption on natural zeolite, modified clinoptilolite with cations, amines and ionic liquids. *Sustainable Chemistry and Pharmacy*, 22 (2021), 100495. <https://doi.org/10.1016/j.scp.2021.100495>
- Panayotova, M. I., Mintcheva, N. N., Gemishev, O. T., Tyuliev, G. T., Gicheva, G. D., & Djerahov, L. P. (2018). Preparation and antimicrobial properties of silver nanoparticles supported by natural zeolite clinoptilolite. *Bulgarian Chemical Communications*, 50, 211–218.
- Ruangtong, J., T-Thienprasert, J., & T-Thienprasert, N. P. (2020). Green synthesized ZnO nanosheets from banana peel extract possess anti-bacterial activity and anti-cancer activity. *Materials Today Communications*, 24(May), 101224. <https://doi.org/10.1016/j.mtcomm.2020.101224>
- Wang, L., Hu, C., & Shao, L. (2017). The antimicrobial activity of nanoparticles: Present situation and prospects for the future. *International Journal of Nanomedicine*, 12, 1227–1249. <https://doi.org/10.2147/IJN.S121956>